General Conditions of Collinearity at the Phase Boundaries of Fluid Mixtures

The general collinearity conditions at phase boundaries for mixtures are proved by thermodynamic identities for density and for entropy as functions of temperature, pressure, and composition. In the case of density/temperature/pressure/composition collinearity is always found at the cricondentherm or any temperature extremum, whereas for entropy/temperature/pressure/composition collinearity is always found at the cricondenbar or any pressure extremum. Qualitative phase diagrams for a typical binary system are presented in accordance with the derived inequalities. Whether a particular slope, involving the above variables, from the homogeneous side of the phase boundary is greater or less than that from the heterogeneous side depends on location on the phase boundary with respect to cricondentherm, critical point, and cricondenbar.

P. T. Eubank, M. A. Barrufet
Texas A&M University
Department of Chemical Engineering
College Station, TX 77843

Introduction

Recently Rowlinson et al. (1986) have proved that fluid isochores are collinear at the cricondentherm (CT) of a binary mixture whereas fluid isoentropes are collinear at the cricondenbar (CB), as in Figure 1. Because the proofs use only thermodynamic identities, they are strictly obeyed by real fluid mixtures. Further, the results of these proofs are easily extended to multicomponent systems via the pseudobinary concept. For example, a proof of isochoric collinearity at the CT for ternary systems is available from the authors.

Collinearity of the isochores at the cricondentherm had been proved earlier by Griffiths in Dorion et al. (1976). Griffiths' proof differs considerably from that of Rowlinson et al. in that it is more concise and mathematical. Because of this conciseness, we repeated a backward version of this proof in Rowlinson et al. Here, we first provide a complementary proof that the jump in $(\partial S/\partial T)_{P,z_i}$ is always negative at the phase boundary. These two basic proofs then allow us to describe the general conditions of collinearity among the variables of temperature T, pressure P, density ρ, composition or mol fraction z, and entropy S. Although a total of 30 collinearity conditions results, only the six associated with $\rho(T, P, z_1)$ and the six associated with $S(P, T, z_1)$ appear to be of practical importance. It is the principal objective of this article to prove these twelve conditions and apply them to common vapor-liquid equilibria (VLE) diagrams, for example, T vs. z_1 at constant P. Of course, the same conditions apply to liquid-liquid and to gas-gas equilibria.

Collinearity conditions and thermodynamic knowledge of the sign of the jump in the slope of the isochore (or isentrope, isobar, or isotherm) at the phase boundary are important for numerous reasons. First, collinearity of the isochores in Figure 1 was discovered originally by experiment (Doiron et al., 1976). The more general application of collinearity concepts of this paper should provide experimenters with valuable qualitative information about how their experiments should come out when passing across phase boundaries. Second, several methods for detection of the phase boundary use a change of slope method. For example, our laboratory (Eubank et al., 1985) uses the change of slope of isochores to detect the lower dew-point curve. At higher densities approaching the cricondentherm, the method fails. It also fails in the zero density limit but can be used again at high densities well above the cricondentherm density. Should we ever measure an isochoric slope greater on the single-phase side of a lower dew-point envelope than on the two-phase side, our data would be thermodynamically impossible. Third, we have shown (Barrufet and Eubank, 1987) these collinearity conditions to be useful to constrain the constants in equations of state (EOS)/mixture combining rules (MCR) for prediction of phase equilibria including the dew-bubble curve (DBC), isochores, and isentropes as in Figure 1. This idea is analogous to the use of the two critical constraints for pure components $[(\partial P/\partial V)_{T_c|CP} = 0 =$

Correspondence concerning this paper should be addressed to P. T. Eubank.

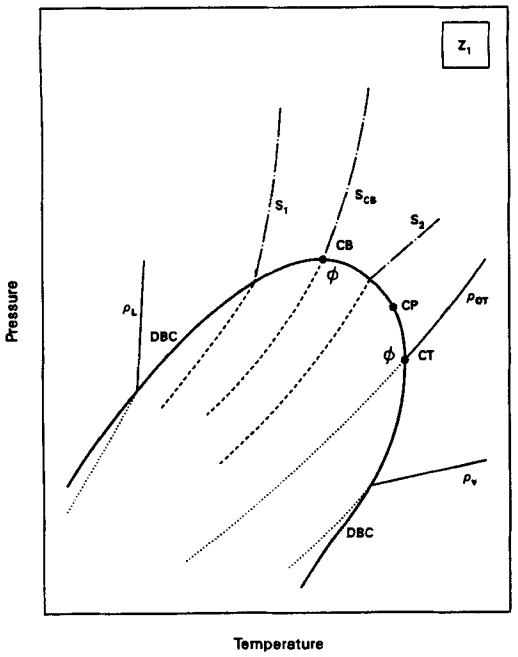

Figure 1. Qualitative pressure/temperature diagram for binary vapor-liquid equilibria.

DBC: Dew-bubble curve, phase boundary enclosing the heterogeneous region. Outer, homogeneous region is termed vapor for densities less than at that the critical point CP, but liquid for higher densities. Density and entropy are monotonic along the DBC. Isochores are collinear, ϕ, at cricondenterm CT; isentropes are collinear at cricondenbar CB.

$(\partial^2 P/\partial V^2)_{T_c|CP}$] to fix the two constants of simple cubic EOS in terms of critical constants. The collinear constraints tie down the assumed EOS/MCR at the CT and at the CB for a mixture. The new density-dependent combining rules (Mansoori and Ely, 1985) are particularly well suited for use with collinearity constraints to provide future VLE calculations with more nearly correct physics.

Specific Collinearity—The Entropy Proof

A standard mathematical argument is employed three times to relate various quantities across the dew-bubble curve (DBC) of Figure 1. Let $\xi(\psi, \omega)$ be a continuous function whose derivatives are discontinuous along a curve in the (ψ, ω) plane separating regions I and II (i.e., I is the single-phase region and II the two-phase region). The differential of ξ along this curve is

$$d\xi = (\partial\xi/\partial\psi)^{\mathrm{I}}_{\omega} d\psi + (\partial\xi/\partial\omega)^{\mathrm{I}}_{\psi} d\omega = (\partial\xi/\partial\psi)^{\mathrm{II}}_{\omega} d\psi + (\partial\xi/\partial\omega)^{\mathrm{II}}_{\psi} d\omega \quad (1)$$

where $(\partial\xi/\partial\psi)^{\mathrm{I}}_{\omega}$ refers to the derivative at the DBC taken from the side of region I, etc. Then

$$[(\partial\xi/\partial\psi)^{\mathrm{I}}_{\omega} - (\partial\xi/\partial\psi)^{\mathrm{II}}_{\omega}] d\psi = -[(\partial\xi/\partial\omega)^{\mathrm{I}}_{\omega} - (\partial\xi/\partial\omega)^{\mathrm{II}}_{\psi}] d\omega \quad (2)$$

or

$$\delta(\partial\xi/\partial\psi)_{\omega} = -(d\omega/d\psi) \cdot \delta(\partial\xi/\partial\omega)_{\psi} \quad (3)$$

where δ indicates the difference, I−II. Griffiths (Dorion *et al.*, 1976) examined a specific form of Eq. 3,

$$\delta(\partial P/\partial\rho)_{T,z_1} = -(dT/d\rho)_{z_1} \cdot \delta(\partial P/\partial T)_{\rho,z_1}, \quad (4)$$

where the total derivative $(dT/d\rho)_{z_1}$ is taken along the DBC, to prove that the lefthand side of Eq. 4 is always nonnegative, so that $\delta(\partial P/\partial T)\rho,z_1$ must be negative below the CT, positive above the CT, and thus zero itself at the CT.

When $S(P, T, z_1)$ replaces $\rho(T, P, z_1)$, analogous arguments can be made. First, the analogous form of Eq. 4 is

$$\delta(\partial T/\partial S)_{P,z_1} = -(dP/dS)_{z_1} \cdot \delta(\partial T/\partial P)_{S,z_1}. \quad (4a)$$

Second, let $\xi \equiv S, \psi \equiv T$, and $\omega = z_1$ (constant P), so that Eq. 3 is

$$\delta(\partial S/\partial T)_{P,z_1} = -(dz_1/dT)_P \cdot \delta(\partial S/\partial z_1)_{P,T} \quad (5)$$

Third,

$$(\partial S/\partial z_1)_{P,T} = \bar{S}_1 - \bar{S}_2 = -(\partial\Delta/\partial T)_{P,z_1} \quad (6)$$

Next, let $\xi \equiv \Delta \equiv \hat{\mu}_1 - \hat{\mu}_2, \psi \equiv T$, and $\omega \equiv z_1$ (constant P), so that Eq. 3 is

$$\delta(\partial\Delta/\partial T)_{P,z_1} = -(dz_1/dT)_P \cdot \delta(\partial\Delta/\partial z_1)_{P,T} \quad (7)$$

Combination of Eqs. 5, 6, and 7 provides

$$\delta(\partial S/\partial T)_{P,z_1} = -(dz_1/dT)^2_P \cdot \delta(\partial\Delta/\partial z_1)_{P,T} \quad (8)$$

Because $\delta(\partial\Delta/\partial z_1)_{P,T} \geq 0, \delta(\partial S/\partial T)_{P,z_1} \leq 0$. Now $(\partial S/\partial T)_{P,z_1} \equiv (C_{Pz}/T) \geq 0$, for thermal stability, so $C^{\mathrm{II}}_{Pz} > C^{\mathrm{I}}_{Pz}$ and $\delta(\partial T/\partial S)_{P,z_1} \geq 0$ to complete the entropy proof.

General Collinearity Equations

We have seen that proof of $\delta(\partial P/\partial\rho)_{P,z_1} \geq 0$ provides collinearity of the isochores in Figure 1 via Eq. 4. Where three independent variables are involved, Eq. 3 can be written as

$$\delta(\partial\xi/\partial\psi)_{\omega,\nu} = -\delta[(\partial\xi/\partial\omega)_{\psi,\nu} \cdot (\partial\omega/\partial\psi)_{\xi,\nu}]$$

$$= -(d\omega/d\psi)_{\nu} \cdot \delta(\partial\xi/\partial\omega)_{\psi,\nu} \quad (9a)$$

$$= -(d\omega/d\xi)_{\nu}(\partial\xi/\partial\omega)^{\mathrm{I}}_{\psi,\nu}(\partial\xi/\partial\omega)^{\mathrm{II}}_{\psi,\nu} \cdot \delta(\partial\omega/\partial\psi)_{\xi,\nu} \quad (9b)$$

Equation 4 is a specific example of this general identity.

For $\rho(T, P, z_1)$ there are six independent forms of $\delta(\partial\xi/\partial\psi)_{\omega,\nu}$ because ξ can be any one of the four variables, ψ any one of the remaining three variables, and reciprocal derivatives are not counted. Likewise, there are six independent forms for $S(P, T, z_1)$. We consider these 12 collinearity conditions below but not the remaining 18 caused by elimination of either T, P, or z_1 from among the five variables (S, ρ, T, P, z_1).

The six (ρ, T, P, z_1) relations are:

$$\delta(\partial P/\partial\rho)_{z_1,T} \geq 0 \quad (10)$$

$$\delta(\partial P/\partial T)_{z_1,\rho} \cdot (dT/d\rho)_{z_1} = -\delta(\partial P/\partial\rho)_{z_1,T} \leq 0 \quad (4)$$

causing $\delta(\partial P/\partial T)_{z_1,\rho} = 0$ at $(dT/d\rho)_{z_1} = 0$.

$$\delta(\partial\rho/\partial z_1)_{P,T} \cdot (dz_1/dP)_T = -\delta(\partial\rho/\partial P)_{z_1,T} \geq 0, \quad (11)$$

causing $\delta(\partial\rho/\partial z_1)_{P,T} = 0$ at $(dz_1/dP)_T = 0$.

$$\delta(\partial\rho/\partial T)_{P,z_1} \cdot (dT/dP)_{z_1} = -\delta(\partial\rho/\partial P)_{z_1,T} \geq 0, \quad (12)$$

causing $\delta(\partial\rho/\partial T)_{P,z_1} = 0$ at $(dT/dP)_{z_1} = 0$.

$$\delta(\partial P/\partial z_1)_{T,\rho} \cdot (dz_1/d\rho)_T = -\delta(\partial P/\partial\rho)_{z_1,T} \leq 0, \quad (13)$$

causing $\delta(\partial P/\partial z_1)_{T,\rho} = 0$ at $(dz_1/d\rho)_T = 0$.

$$\delta(\partial T/\partial z_1)_{P,\rho} \cdot (dz_1/d\rho)_P = -\delta(\partial T/\partial\rho)_{P,z_1} = (dP/dT)_{z_1}(\partial T/\partial P)^{\mathrm{I}}_{\rho,z_1}(\partial T/\partial P)^{\mathrm{II}}_{\rho,z_1} \cdot \delta(\partial P/\partial\rho)_{z_1,T} \quad (14a)$$

or,

$$\delta(\partial T/\partial z_1)_{P,\rho}(dz_1/d\rho)_P(dT/dP)_{z_1}(\partial P/\partial T)^{\mathrm{I}}_{\rho,z_1}(\partial P/\partial T)^{\mathrm{II}}_{\rho,z_1} = \delta(\partial P/\partial\rho)_{z_1,T} \geq 0. \quad (14b)$$

If $(\partial P/\partial T)^{\mathrm{I}}_{\rho,z_1}$ and $(\partial P/\partial T)^{\mathrm{II}}_{\rho,z_1}$ are assumed to be nonzero and of the same sign (see Figure 1),

$$\delta(\partial T/\partial z_1)_{P,\rho}(dz_1/d\rho)_P(dT/dP)_{z_1} \geq 0 \quad (14c)$$

causing $\delta(\partial T/\partial z_1)_{P,\rho} = 0$ at $(dz_1/d\rho)_P(dT/dP)_{z_1} = 0$.

The six (S, P, T, z_1) relations are analogously:

$$\delta(\partial T/\partial S)_{z_1,P} \geq 0 \quad (15)$$

$$\delta(\partial T/\partial P)_{z_1,S} \cdot (dP/dS)_{z_1} = -\delta(\partial T/\partial S)_{z_1,P} \leq 0, \quad (16)$$

causing $\delta(\partial T/\partial P)_{z_1,S} = 0$ at $(dP/dS)_{z_1} = 0$.

$$\delta(\partial S/\partial z_1)_{T,P}(dz_1/dT)_P = -\delta(\partial S/\partial T)_{z_1,P} \geq 0, \quad (17)$$

causing $\delta(\partial S/\partial z_1)_{T,P} = 0$ at $(dz_1/dT)_P = 0$.

$$\delta(\partial S/\partial P)_{T,z_1}(dP/dT)_{z_1} = -\delta(\partial S/\partial T)_{z_1,P} \geq 0, \quad (18)$$

causing $\delta(\partial S/\partial P)_{T,z_1} = 0$ at $(dP/dT)_{z_1} = 0$.

$$\delta(\partial T/\partial z_1)_{P,S}(dz_1/dS)_P = -\delta(\partial T/\partial S)_{z_1,P} \leq 0, \quad (19)$$

causing $\delta(\partial T/\partial z_1)_{P,S} = 0$ at $(dz_1/dS)_P = 0$.

$$\delta(\partial P/\partial z_1)_{T,S} \cdot (dz_1/dS)_T = -\delta(\partial P/\partial S)_{T,z_1} = (dT/dP)_{z_1}(\partial P/\partial T)^{\mathrm{I}}_{S,z_1}(\partial P/\partial T)^{\mathrm{II}}_{S,z_1} \cdot \delta(\partial T/\partial S)_{z_1,P} \quad (20a)$$

or,

$$\delta(\partial P/\partial z_1)_{T,S}(dz_1/dS)_T(dP/dT)_{z_1}(\partial T/\partial P)^{\mathrm{I}}_{S,z_1}(\partial T/\partial P)^{\mathrm{II}}_{S,z_1} = \delta(\partial T/\partial S)_{z_1,P} \geq 0. \quad (20b)$$

If $(\partial T/\partial P)^{\mathrm{I}}_{S,z_1}$ and $(\partial T/\partial P)^{\mathrm{II}}_{S,z_1}$ are assumed to be nonzero and of the same sign, see Figure 1,

$$\delta(\partial P/\partial z_1)_{T,S}(dz_1/dS)_T(dP/dT)_{z_1} \geq 0, \quad (20c)$$

causing $\delta(\partial P/\partial z_1)_{T,S} = 0$ at $(dz_1/dS)_T(dP/dT)_{z_1} = 0$.

Applications to Phase Diagrams

Equations 4 and 10–20c are written with the understanding that ρ and S behave monotonically when proceding along a phase boundary. Thus the collinearity of Eq. 4 occurs at $dT = 0$, a cricondentherm, whereas the collinearity of Eq. 16 occurs at $dP = 0$, a cricondenbar, as shown in Figure 1. Indeed, all six collinearity conditions originating from (ρ, T, P, z_1) result in collinearity at the cricondentherm whereas the six collinearity conditions originating from (S, P, T, z_1) result in collinearity at the cricondenbar. We now examine the qualitative features of individual (ρ, T, P, z_1) diagrams. Like the equations of the previous section, the individual (S, P, T, z_1) diagrams are qualitatively similar to the corresponding (ρ, T, P, z_1) diagrams upon interchange of P with T plus S with ρ.

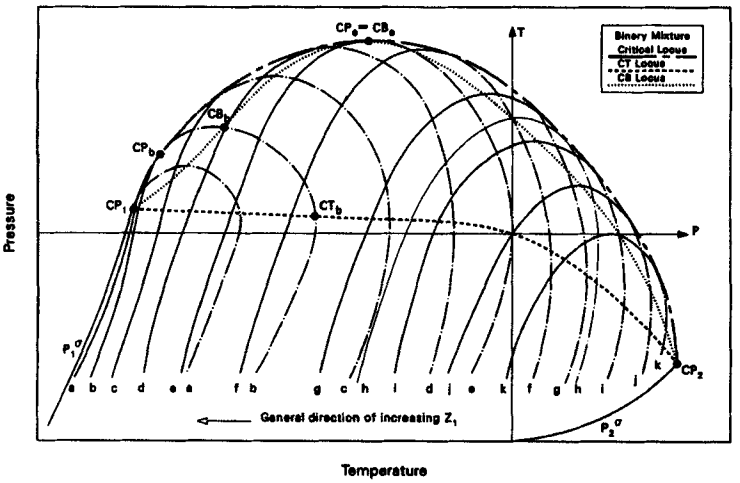

Figure 2. Detailed pressure/temperature diagram.

a–k. Sequence of convoluted isopleths or DBC

Figures 3–8 refer to this binary system; those drawn at constant T or P refer to T or P marked here

For consistency, all of the diagrams to follow are taken from the binary VLE system of Figure 2, a P/T diagram containing

1. The critical, CT, and CB locii
2. The series of convoluted DBC (or isopleths) of different constant compositions

Figure 2 is typical of simple hydrocarbon mixtures where component 1 is the more volatile, $T_{c2} > T_{c1}$, $P_{c1} > P_{c2}$, and the critical locus is complete. Later diagrams for constant T (or P) refer specifically to the isotherm (or isobar) marked in Figure 2.

Figure 1 has shown already the collinearity of isochores at the CT of Eq. 4. Another diagram of constant overall composition z_1 is Figure 3, pressure vs. density showing isotherms. Equation 10 demands that the isothermal slope on the single-phase side of the DBC be greater or equal to the corresponding slope on the two-phase side. Further, all slopes in this diagram must be positive for mechanical stability. Consistent with Figure 2, $T_{CT} > T_C > T_{CB}$ in Figure 3. Collinearity exists only in the trivial sense that the isotherm of maximum temperature T_{CT} is tangent to the dew-point curve at the cricondentherm pressure or $\delta(\partial P/\partial\rho)_{z_1,T}$ is zero only at the CT.

Figure 4 is similar to a volume ($V = \rho^{-1}$) vs. composition diagram appearing recently in Rowlinson and Swinton (1982, p. 197). This figure shows a sequence of isobars all at the constant temperature marked in Figure 2. There we see that $P_c > P_{CB} > P_{CT}$. Equation 11 provides the collinearity condition that

$$(dz_1/dP)_T \cdot \delta(\partial V/\partial z_1)_{P,T} \leq 0. \tag{21}$$

Starting at low densities (high volumes) on the dew-point curve of Figure 4 and moving to ever higher densities, we find that $(dz_1/dP)_T$ is positive until the cricondentherm volume is reached. At this point $(dz_1/dP)_T$ diverges to positive infinity, returning from negative infinity for volumes less than that at the cricondentherm. Thus for the isobar P_1, at the dew point

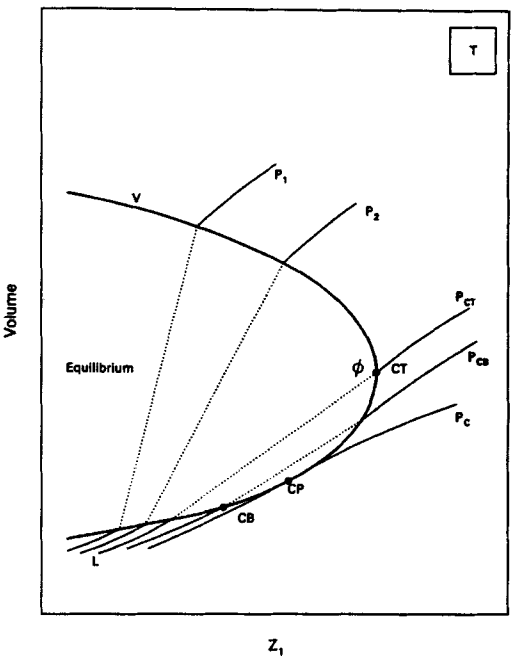

Figure 4. Volume/composition diagram for fixed temperature.

Isobars are similar to those of Rowlinson and Swinton (1982) Isobaric collinearity is observed at the CT, which is also the extremum of z_1; isobars are straight equilibrium tie lines in the two-phase region

$(\partial V/\partial z_1)^{II}_{P,T} > (\partial V/\partial z_1)^{I}_{P,T}$, as shown in Figure 4. At the cricondentherm, the isobar P_{CT} is collinear. Next, the isobar P_{CB} crosses the dew-point curve between the CT and CP. Physically, this point represents the vapor in equilibrium with the liquid of the cricondenbar locus of Figure 2. For this vapor,

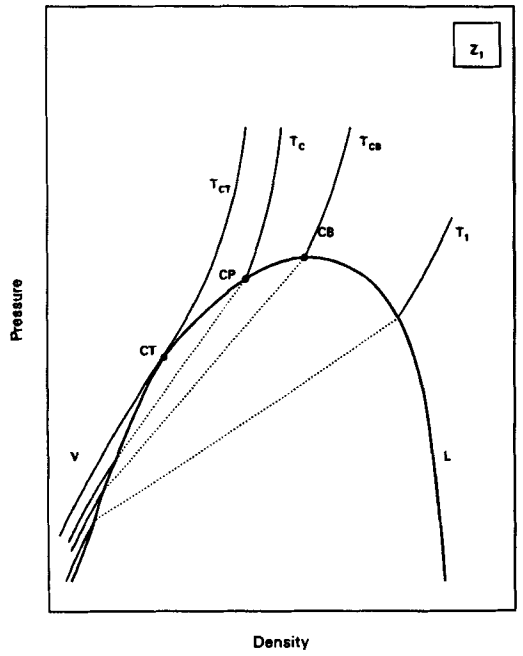

Figure 3. Pressure/density diagram for fixed composition.

Collinearity at CT is trivial

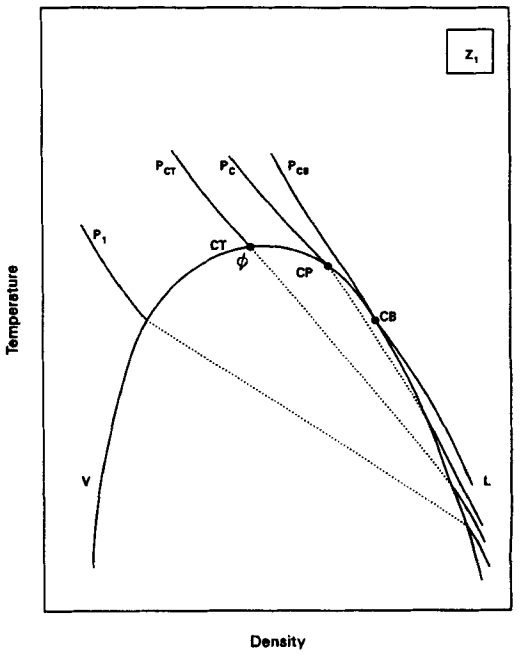

Figure 5. Temperature/density diagram: isobars at constant composition.

$\delta(\partial V/\partial z_1)_{P,T} < 0$. At the CP, the pressure reaches its maximum value P_c and $\delta(\partial V/\partial z_1)_{P,T} = 0$, a trivial collinearity condition in that the critical isobar is tangent to the DBC. For volumes less than critical, $(dz_1/dP)_T$ is again positive and $\delta(\partial V/\partial z_1)_{P,T} < 0$ all along the bubble-point curve of Figure 4 including the cricondenbar, CB.

Next, we examine the qualitative feature of Figure 5, the popular T/ρ diagram at constant composition with P as the parameter. The collinearity condition is Eq. 12: $(dT/dP)_{z_i} \cdot \delta(\partial\rho/\partial T)_{P,z_1} \geq 0$. Along the DBC, $(dT/dP)_{z_1}$ is positive at low densities, passing zero at the CT to become negative between the CT and CB. At the CB it diverges to negative infinity, returning from positive infinity at densities slightly above that at the CB. Now $\delta(\partial\rho/\partial T)_{P,z_1}$ has the same sign as $(dT/dP)_{z_1}$, or $\delta(\partial T/\partial\rho)_{P,z_1}$ has the opposite sign. Thus, $(\partial T/\partial\rho)^{II}_{P,z_1} > (\partial T/\partial\rho)^{I}_{P,z_1}$ for low densities until they are equal at the CT. This inequality is reversed between CT and CB, for example, at the CP. $\delta(\partial T/\partial\rho)_{P,z_1}$ is zero at CB, with the critical isobar tangent to the bubble-point curve. For all saturated liquids of density above that at CB, the isobar slope on the heterogeneous side again exceeds that on the homogeneous side of the bubble-point curve.

Figure 6 is the common pressure/composition diagram resulting from VLE measurements at constant temperature. Here, however, the isochores from P-T-V-z_1 data are shown. The isotherm for Figure 6 is that marked in Figure 2 and used previously for Figure 4. The collinearity condition, Eq. 13, shows the sign of $\delta(\partial P/\partial z_1)_{T,\rho}$ to be opposite to that of $(dz_1/d\rho)_T$. This latter slope is positive at low densities but zero at the cricondencomp (CC), which is physically a cricondentherm at the temperature fixed for Figure 6. To understand why CC points on P/z_1 diagrams are also cricondentherms, we return to Figure 2 along the marked isotherm. The intersection of this isotherm with the

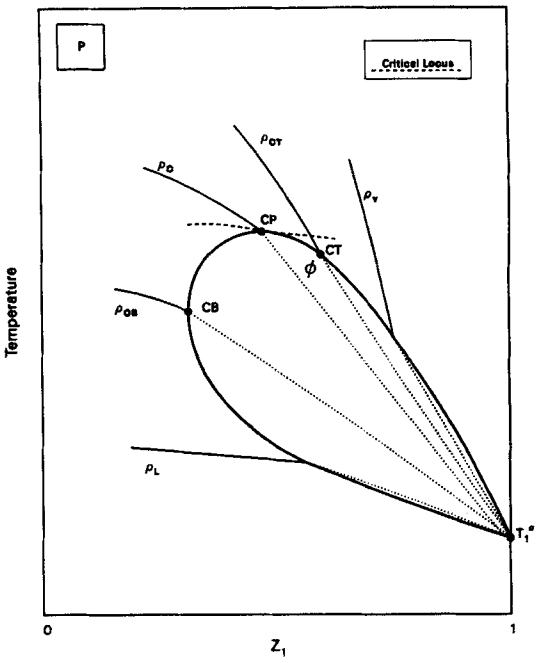

Figure 7. Temperature/composition diagram: isochores at constant pressure.

CT locus provides a vapor of the maximum composition z_1 that can coexist with a liquid (of composition corresponding to the bubble-point curve also passing through the T/CT locus intersection). Any pressure above or below that of the CT locus at T will result in a saturated vapor mixture of mole fraction less than this z_1. Returning to Figure 6, $(dz_1/d\rho)_T$ is negative between the CC and the density of pure saturated liquid 2 (at $z_1 = 0$). Thus,

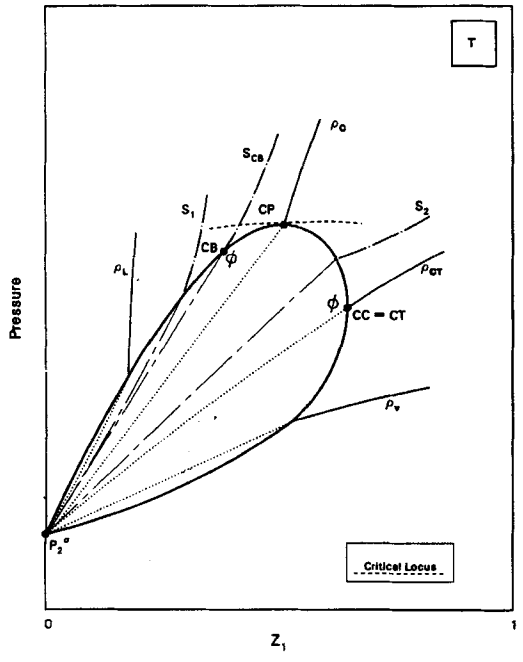

Figure 6. Pressure/composition diagram: isochores and isentropes at constant temperature.

Extremum in z_1 (cricondencomp CC) is a cricondentherm point similar to Figure 4.

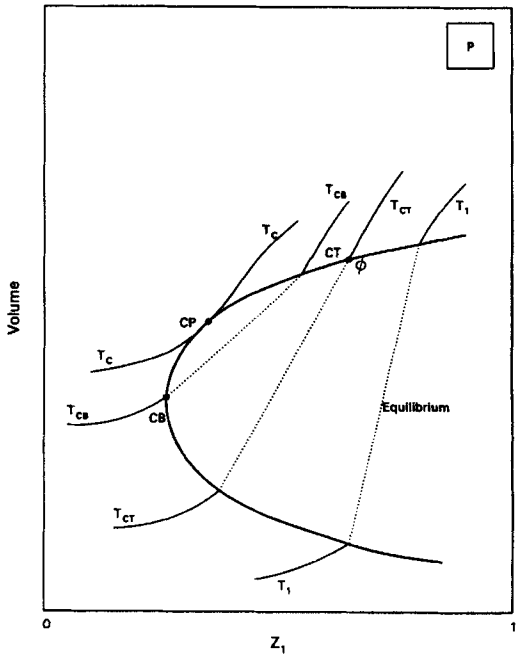

Figure 8. Volume/composition diagram: isotherms at constant pressure for use with Figure 7.

Collinearity condition and inequality equation for $\delta(\partial V/\partial z_1)_{T,P}$ are common to Figure 4

$\delta(\partial P/\partial z_1)_{T,\rho}$ is negative from low densities to the CC density, zero at the CC density, and positive at higher densities including the critical density.

Figure 7 is the common temperature/composition diagram resulting from VLE measurements at constant pressure. The isobar for Figure 7 is that marked in Figure 2 and used later for Figure 8. The collinearity condition, Eq. 14c, shows the sign of $\delta(\partial T/\partial z_1)_{P,\rho}$ to be the same as that of the $(dz_1/d\rho)_P\,(dT/dP)_{z_1}$ product. $(dz_1/d\rho)_P$ is negative at low densities, Figure 7, but increases with density to zero at the CB and is positive for $\rho > \rho_{CB}$. However, $(dT/dP)_{z_1}$ is positive at low densities, Figure 1, decreases to zero at the CT, is negative from ρ_{CT} to ρ_{CB}, diverges to negative infinity at the CB ($\rho < \rho_{CB}$), and returns from positive infinity to the left of the CB to be positive at the higher densities. The product $(dz_1/d\rho)_P\,(dT/dP)_{z_1}$ is then

1. Negative at low densities to the CT
2. Zero at the CT
3. Positive from the CT past the CB to higher densities

The cricondencomp (CC) of Figure 7 is physically a cricondenbar at the pressure fixed for Figure 7. This result is understood upon examination of the marked isobar of Figure 2. The intersection of this marked isobar with the CB locus provides the minimum z_1 value (maximum z_2) at which the saturated liquid can exist under the marked pressure. Returning to Figure 7, collinearity of the isochores is seen at the CT but not at the CP nor CB(CC).

Figure 8 is a V/z_1 diagram at constant pressure showing isotherms. It is a mate to Figure 7 in that both are for constant pressure. However, it is also closely related to Figure 4 due to sharing Eq. 21 as a collinearity condition. Equation 21 can be written as

$$(dz_1/dT)_P(dT/dP)_{z_1} \cdot \delta(\partial V/\partial z_1)_{P,T} \geq 0, \qquad (24)$$

where $(dT/dP)_{z_1}$ is evaluated from Figure 1 as above and $(dz_1/dT)_P$ is best seen in Figure 7. $\delta(\partial V/\partial z_1)_{P,T}$ is thus

1. Negative from low densities to the CT
2. Zero at the CT
3. Positive from the CT to CP where $(dz_1/dT)_P$ is zero
4. Continues negative for $\rho > \rho_{CB}$

The above diagrams form a set consistent with the V/z_1 diagram at constant T of Rowlinson and Swinton (1982). By increasing the marked pressure of Figure 2 to exceed the critical pressure of both pure components, the reader can form a more entertaining set of phase diagrams. Figures 7 and 8 will exhibit two-phase islands with two critical points and two cricondenbars, corresponding to the extrema in z_1. As the cricondentherm locus is drawn in Figure 2, no CT points and hence no collinearity would be observed in Figure 7 and 8. However, if the cricondentherm locus of Figure 2 were to rise above the critical pressure of pure 1 and achieve a maximum itself, then double CT points would occur on the islands for $P_{C1} < P <$ maximum pressure of the cricondentherm locus. These systems represent simple hydrocarbon mixture behavior; even more entertaining diagrams result from azeotropic systems, both positive and negative. The reader can apply the inequalities and collinearity notions of this work to any phase boundary regardless of the number of components in the mixture or the molecular complexities of the solutions.

Acknowledgment

Financial suport by the National Science Foundation, Grant No. CBT-8420547, is gratefully acknowledged. We also thank K. R. Hall, J. C. Holste, and J. S. Rowlinson for helpful advice.

Notation

CB = cricondenbar or extremum of pressure along phase boundary
CC = cricondencomp or extremum of mole fraction along phase boundary
CP = critical point on phase boundary
CT = cricondentherm or extremum of temperature along phase boundary
C_{pz} = isobaric heat capacity for a mixture or $T\,(\partial S/\partial T)_{p,z_1}$
DBC = a dew-bubble curve (or isopleth)
G_m = molar Gibbs energy of mixture
P = absolute pressure
L = liquid (in diagrams)
S = molar entropy of mixture
S_i = partial molar entropy of component i in mixture
T = absolute temperature
V = molar volume of mixture
V = vapor (in diagrams)
z_1 = overall mole fraction of component 1 in binary mixture

Greek letters

Δ = difference of chemical potentials in binary mixture, $\hat{\mu}_1 - \hat{\mu}_2$
δ = jump discontinuity of a thermophysical property at phase boundary; here, the single-phase side value (I) less that from the two-phase side (II)
$\hat{\mu}_i$ = chemical potential of component i in mixture
ν = general independent variable, Eq. 13
ξ = general dependent variable, Eq. 1
ρ = molar density of mixture or V^{-1}
ϕ = collinearity position as noted in phase diagrams
ψ = general independent variable, Eq. 1
ω = general independent variable, Eq. 1

Subscripts

c = critical value

Superscripts

I = single-phase value at phase boundary
II = two-phase value at phase boundary

Literature Cited

Barrufet, M. A., and P. T. Eubank, "New Physical Constraints for Fluid Mixture Equations of State and Mixture Combining Rules," Spring Nat. Meet. AIChE, Houston (1987); also to appear in *Fluid Phase Equilibria.*

Doiron, T., R. P. Behringer, and H. Meyer, "Equation of State of a ^{3}He-^{4}He Mixture Near Its Liquid-Vapor Critical Point," *J. Low Temp. Phys.*, **24**(3/4), 345 (1976).

Eubank, P. T., A. Kreglewski, K. R. Hall, J. C. Holste, and H. Mansoorian, "Density of an Equimolar Mixture of Ethane and Methyl Chloride," *AIChE J.*, **31**(5), 849 (1985).

Mansoori, G. A., and J. F. Ely, "Density Expansion (DEX) Mixing Rules: Thermodynamic Modeling of Supercritical Extraction," *J. Chem. Phys.*, **82**(1), 406 (1985).

Rowlinson, J. S., and F. L. Swinton, *Liquids and Liquid Mixtures,* 3rd ed., Butterworths, London (1982).

Rowlinson, J. S., G. J. Esper, J. C. Holste, K. R. Hall, M. A. Barrufet, and P. T. Eubank, "The Collinearity of Isochores at Single- and Two-Phase Boundaries for Fluid Mixtures," *Equations of State: Theory and Applications,* K. C. Chao, R. L. Robinson, Jr., eds., ACS Symp. Ser. 300, Am. Chem. Soc., Washington, ch. 2 (1986).

Manuscript received Nov. 21, 1986, and revision received Apr. 14, 1987.